2026 IEEE International Conference on Robotics and Automation (ICRA 2026)
June 1-5, 2026. Vienna, Austria

TetherBot: A Power-Tethered sUAS Platform for Autonomous Vertical Atmospheric Profiling

Daniel A. Rico[1,5], Francisco Muñoz-Arriola[3,4,5], and Justin M. Bradley[2,6]

***Abstract*— Resolving vertical gradients of atmospheric variables in agroecosystems is essential for understanding surface-atmosphere exchange. It is also critical for emerging carbon monitoring frameworks. Existing methods, such as eddy covariance towers and satellite remote sensing, provide observations with limited spatial resolution, leaving fine-scale structure undersampled. This work introduces TetherBot, a tethered robotic profiler integrated into the Tethered Aircraft Uncrewed System. The robot traverses a hoisted power tether, enabling persistent vertical profiling with synchronized sensing and telemetry. Field experiments across a 40 m transect demonstrated reliable operation. Barometric pressure provided consistent altitude, temperature resolved subtle stratification, and relative humidity revealed surface-layer variability. Carbon dioxide measurements were dominated by sensor noise, highlighting the need for higher-fidelity analyzers. These results demonstrate the feasibility of tethered robotic profiling as a viable approach for atmospheric monitoring. They establish a foundation for future multi-robot arrays and high-precision flux applications.**

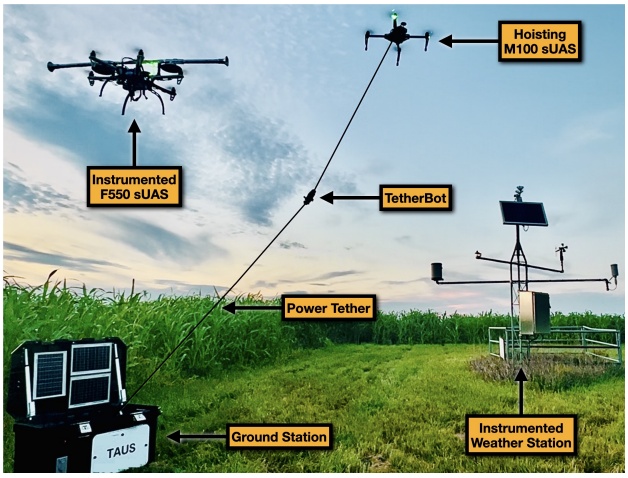

Fig. 1: TetherBot traverses the hoisted power tether of the TAUS while proximal assets provide reference measurements in the wild.

I. Introduction

Agroecosystems in particular can function as both sources and sinks of greenhouse gases such as methane (CH_4) and carbon dioxide (CO_2), depending on management practices and environmental drivers [1], [2]. Verification of carbon sequestration is therefore not only a scientific necessity but also an economic one, ensuring that carbon credit markets rest on robust and defensible measurements. However, current measurement infrastructures remain limited. Eddy covariance (EC) towers provide high-frequency and high-fidelity flux measurements but only at fixed locations and with well-documented energy balance closure challenges [3]. Satellites extend coverage but with limited spatial and temporal resolution for resolving fine-scale atmospheric variability [4]. Small Uncrewed Aerial Systems (sUAS) have been explored but remain constrained. Fixed-wing sUAS offer coverage and multi-rotors can hover; however, both have limited flight times due to battery constraints [5]. Conventional approaches mount sensors directly on the sUAS, which introduces measurement challenges that can bias atmospheric observations. Sensors on multi-rotors are exposed to propeller wash, thermal bias, and electromagnetic interference, degrading measurement fidelity. These effects can be partially mitigated through careful mechanical design, such as aspirated inlets and extended sensor housings [6]. Such mitigation requires non-trivial, platform-specific integration and careful aerodynamic design. As a result, traditional sUAS remain limited in their ability to support sustained vertical profiling of the near-surface boundary layer. To address these challenges, we leverage a hoisted power-tethered robotic sensing platform, referred to as the Tethered Aircraft Uncrewed System (TAUS), and introduce a compact mobile agent called TetherBot, capable of autonomous locomotion and sensing along the tether. This configuration enables persistent, *in situ* profiling with synchronized environmental sensing and real-time telemetry. Unlike static towers or short-lived drones, the TetherBot can traverse the tether repeatedly over extended durations, providing a new window into dynamic gradients of pressure, temperature, humidity (PTH), and CO_2 within agroecosystems (see Fig. 1). The key insight of this work is that a sUAS-hoisted power tether can serve not only as an energy conduit but also as a robotic guideway, enabling persistent vertical mobility for environmental sensing. This work advances both field robotics and environmental monitoring. The main contributions are:

1) **A novel tether-traversing robotic platform** capable of vertical mobility along a sUAS-hoisted power tether.
2) **An integrated mechatronic architecture** for autonomous locomotion and atmospheric sensing.
3) **Field experiments demonstrating robotic** vertical profiling across a 40 m atmospheric transect.

This work was supported in part by USDA 2023-67021-38977, NSF-2514761, NSF-2221648, and NASA-ULI-80NSSC20M0162. Conceptual elements were also supported by the Agriculture and Food Research Initiative, Grant 2023-67021-38977, Accession 1029656, through the Cyber-Physical Systems program. [1]School of Computing, [2]Department of Computer Science, [3]School of Natural Resources, [4]Department of Biological Systems Engineering, [5]University of Nebraska–Lincoln, NE, USA, [6]North Carolina State University, NC, USA. Emails: daniel.rico05@huskers.unl.edu, fmunoz@unl.edu, jmbradley@ncsu.edu

A mechanically decoupled mobile sensing platform avoids sUAS-induced perturbations by sampling air away from the aerial vehicle. More importantly, this decoupling transforms the system architecture by removing the tight coupling between sensing fidelity and aerial vehicle dynamics. This enables improved measurement quality and an extensible, scalable multi-agent architecture. Rather than a single payload constrained by the aerial platform, multiple robotic agents can operate parallelized along the tether. This facilitates concurrent vertical profiling and increased sensing throughput beyond even carefully engineered single-platform sUAS deployments. TetherBot thus complements EC towers and existing carbon monitoring infrastructure. Future extensions, including coordinated multi-robot arrays and integration with closed-path analyzers, will further support flux measurements and energy-balance closure. More broadly, this work reframes aerial environmental sensing as a distributed robotic systems problem rather than a single-platform sensing task.

II. Related Work

This section reviews prior work on robotic environmental sensing, tethered aerial systems, cable-riding locomotion, and atmospheric gas sensing, thereby positioning TetherBot as a hybrid platform for persistent vertical profiling along a tethered infrastructure.

A. Robotic Environmental Sensing Platforms

Environmental monitoring has traditionally relied on static infrastructure such as EC flux towers and fixed meteorological stations [7]. More recently, robotic platforms have enabled mobile environmental sensing with expanded spatial coverage [8]. Autonomous ground vehicles, floating sensors [9], and sUAS [10] have been explored for ecological monitoring, though these platforms often remain constrained by endurance and stability. TetherBot instead provides a persistent tethered sensing platform capable of sustained vertical profiling.

B. Tethered Aerial Systems and Hybrid sUAS Platforms

Tethered platforms have emerged as viable systems for persistent aerial operation due to advances in power delivery and data transmission through tether lines [11]. These systems provide continuous power and stable communication links, enabling long-duration sensing deployments [12]. Prior robotic implementations primarily mount sensing payloads directly on the sUAS platform. In contrast, TetherBot treats the tether itself as an active sensing axis, enabling a mobile robot to reposition along the line to sample vertical gradients.

C. Robotic Mobility Along Cables or Rails

Cable-riding robots have been explored for applications such as power line inspection [13] and bridge cable repair [14]. These systems typically operate on rigid, well-defined cables or rails in structured environments. In contrast, TetherBot traverses a flexible power tether suspended beneath a sUAS in open-field conditions, where wind loading and atmospheric disturbances introduce additional motion and variability. These conditions impose different design constraints than traditional cable-climbing robots, requiring lightweight construction and stable traversal along a moving flexible line.

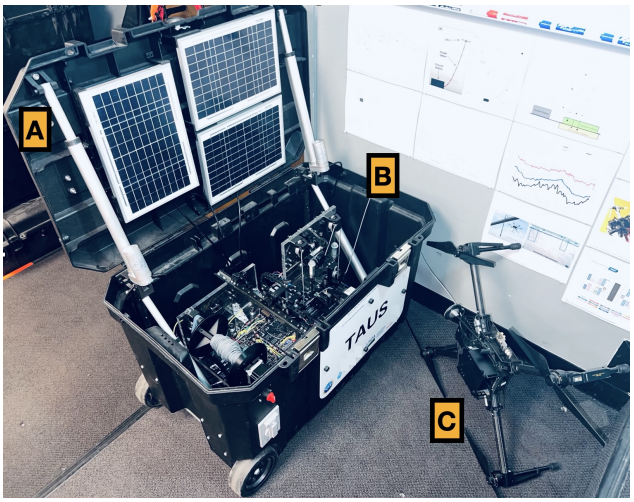

Fig. 2: TAUS is a field-deployable robotic platform composed of subsystems: (A) Ground Station, (B) Power Tether, and (C) sUAS.

D. Atmospheric Gas Monitoring Techniques

High-quality measurements of CO_2, water vapor, and related scalars are typically obtained from stationary systems such as infrared gas analyzers on meteorological or EC towers, offering high precision but limited spatial coverage. Portable nondispersive infrared (NDIR) sensors enable deployment on mobile platforms [15], though compact analyzers trade off accuracy, stability, and response time under size, weight, and power (SWaP) constraints. Active aspiration reduces diffusion lag and improves sampling fidelity. Recent work integrates lightweight CO_2 sensors into sUAS [16], using inlet-based or aspirated designs to mitigate rotor downwash and solar heating. However, these approaches remain constrained by limited endurance and platform-induced perturbations. In contrast, TetherBot embeds aspirated NDIR sensing within a persistent tethered robotic platform for sustained vertical profiling. Although compact NDIR sensors remain noise-limited, this architecture enables integration of higher-fidelity closed-path analyzers for future surface–atmosphere exchange studies.

While prior systems have explored tethered sUAS sensing, cable-climbing robots, and mobile atmospheric sensors independently, no prior work *to our knowledge* integrates a tether-traversing robot with a sUAS-hoisted power tether for persistent vertical profiling. TetherBot addresses this gap by transforming the tether into a robotic sensing axis.

III. Approach

This section outlines the TAUS (see Fig. 2) and the development of its tether-traversing robotic agent, TetherBot. Together they form a heterogeneous multi-robot system for persistent vertical profiling of the lower atmosphere. A power-delivering tether serves both as an energy conduit and

as a robotic guideway along which TetherBot traverses to collect atmospheric measurements. The following subsections describe the system architecture, the TetherBot mechatronic design, integrated sensing capabilities, and the embedded control framework enabling autonomous operation.

A. TAUS Platform Overview

The TAUS platform [17], [18], [19] consists of three primary subsystems: a ground station providing power delivery and system coordination, a power-delivering tether, and a hoisting sUAS that maintains tether elevation. Continuous power delivery enables long-duration environmental monitoring deployments.

1) Ground Station: The ground station provides electrical power regulation and tether management. A battery bank feeds a step-up power supply that delivers energy through the tether. A base computing unit issues high-level commands, receives sensor data, and communicates with both the aerial and mobile components. Redundant telemetry links enable monitoring and intervention, while safety interlocks support emergency tether retrieval and system shutdown.

2) Power Tether: The tether is a lightweight jacketed composite cable that delivers power to airborne components. It contains multi-stranded copper conductors for electrical transmission. Beyond power delivery, the tether functions as a mechanical guideway for TetherBot locomotion, making its structural integrity and sway characteristics important for both flight stability and robotic traversal.

3) sUAS (Hoisting Vehicle): A multi-rotor sUAS elevates and stabilizes the tether. Using onboard Global Navigation Satellite System (GNSS) and inertial feedback, the vehicle maintains position under low to moderate wind conditions while compensating for tether tension and environmental disturbances. The sUAS functions solely as a tether elevator and anchor, with sensing tasks performed by the TetherBot.

B. TetherBot Mechatronic Design

The TetherBot (see Fig. 3) is a compact robotic platform capable of two-degree-of-freedom locomotion along and about the power tether. The platform measures approximately 170 mm $\times$ 115 mm $\times$ 60 mm and has a total mass of 250 g, reflecting design constraints for lightweight operation on a flexible tether. Rather than introducing a new cable-traversal modality, the system employs a friction-driven clamping mechanism that enables reliable motion along a wind-perturbed tether. A lightweight chassis minimizes payload strain while paired drive modules provide bidirectional climbing and intrinsic mechanical clamping for position holding. The platform integrates low-power computing via an 8-bit ATMEGA328P microcontroller unit (MCU), power management, and wireless communication, with synchronized telemetry supporting sensor integration and control.

1) Structural Frame and Pinch Actuation: The structural frame is fabricated from lightweight 3D-printed polymer with embedded fasteners to provide rigidity without excessive mass. It houses both the drivetrain and sensing payloads while distributing loads along the tether to minimize twisting or bending. Locomotion is achieved through a pinch actuation system in which roller assemblies maintain continuous contact with the tether through the fixed geometry of the chassis and are driven by micro-geared motors via spur gear trains. This configuration provides stable traction while accommodating small diameter variations or misalignment. Pinch actuation also provides passive safety. When power is removed, the fixed clamping geometry holds the tether and prevents unintended sliding. Tether release is achieved by driving the rollers with the same geared motors until the tether is fed completely through the mechanism. The mechanical design permits the robot to rotate about the tether as the two clamped drive modules operate and interact with the cable. In the present implementation, this rotational degree of freedom is not actively controlled to achieve specific angles, and any rotation observed results from mechanical asymmetry or cable torsion rather than commanded orientation. These mechanisms provide a stable holding force and controlled traversal along the shared tether.

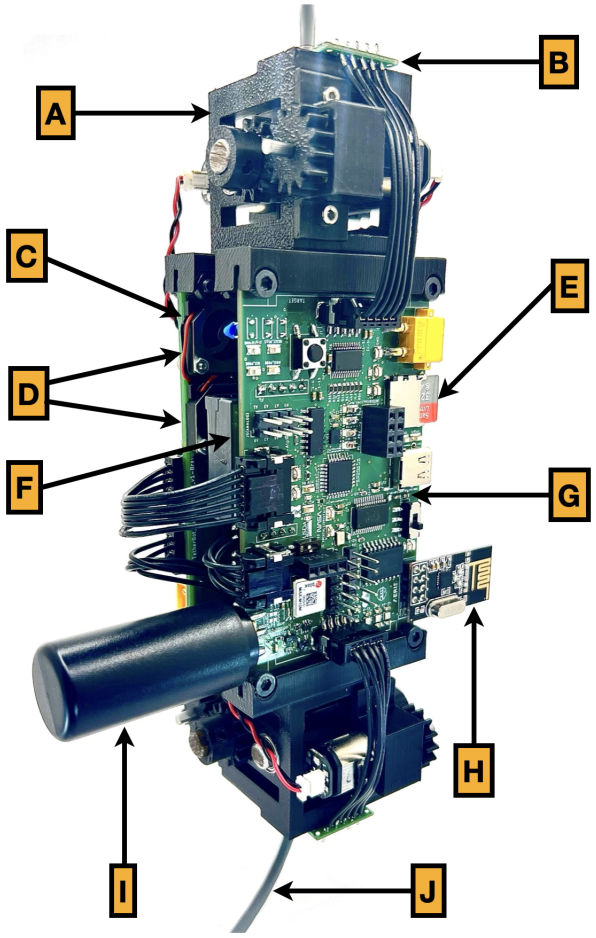

Fig. 3: TetherBot: a tether-traversing robotic platform for atmospheric sampling. (A) Pinch-actuation drivetrain, (B) LiDAR, (C) Daughterboard (rear), (D) Micro-blowers, (E) MicroSD, (F) NDIR CO_2, (G) Motherboard, (H) Telemetry, (I) GNSS, (J) Power tether.

2) Drivetrain: Locomotion is provided by four Pololu micro metal gearmotors (6V, 50:1 ratio, 270 RPM no load, 0.44 kg·cm stall torque). Two independent drive modules

TABLE I: Summary of integrated TetherBot sensors. The redundancy column reflects the number of units co-located on the TetherBot. Data rate refers to the nominal sampling or transmission frequency to balance accuracy, power consumption, and MCU serial bus utilization.

Sensor	Variable	Accuracy	Response Time	Redundancy	Data Rate
IMU (LSM6DSO, 6-axis)	Accel., Angular vel.	± 0.01 g, $\pm 0.1^\circ$/s	< 1 ms	1	50-100 Hz
Thermistor (20kΩ)	Temperature	$\pm 0.5\%$ tol.	< 1 s (air)	3	1-10 Hz
Bosch BMP581	Pressure/Altitude	± 0.5 Pa ($\sim$4 cm)	$\sim$10 ms	3	1-10 Hz
Sensirion SHT45	Relative Humidity	$\pm 1.0\%$ RH	$\sim$8 s (diffusion)	3	1-10 Hz
SenseAir Sunrise	CO_2 concentration	$\pm$(5% reading+30 ppm)	$\sim$30-60 s (diffusion)	1	0.1-1 Hz
nRF24L01+	2.4 GHz wireless comms	—	—	1	10-20 Hz packets
u-blox MAX-M10M	GNSS position, time	< 1 m (SBAS)	1 s	1	1 Hz (PVT), 1 Hz PPS

clamp the tether via spur gear-driven pinch rollers. To estimate climbing capacity, we model the robot as a vertical load with mass M, gravity g, and roller radius $R \approx 3$ mm. Including a 20% friction margin, the required force per motor

$$F = \frac{1.20Mg}{4}, \text{with torque } \tau = FR = \frac{1.20MgR}{4}.$$

For $M = 0.25$ kg, this yields $F \approx 0.736$ N and $\tau \approx 2.21$ mN·m, corresponding to $\sim$51% of the motor stall torque (4.3 mN·m) and providing meaningful climbing margin. Motor current scales with torque from 40 mA (no load) to 360 mA (stall). Assuming a linear scaling, at $\sim$51% load, the current draw is $I \approx 40 + 0.51(360 - 40) \approx 204.3$ mA per motor, giving $\sim$817 mA total on the 6 V rail. The corresponding motor power is $P \approx 6 \times 0.817 \approx 4.90$ W. With an 11.1 V, 450 mAh LiPo battery, the equivalent ideal battery current is $I_{\text{bat}} \approx P/11.1 \approx 0.44$ A, giving

$$t = \frac{0.45 \text{ Ah}}{0.44 \text{ A}} \approx 1.02 \text{ h},$$

or $\sim$49 minutes assuming 80% usable capacity. This drivetrain only runtime estimate represents a conservative upper bound, as it assumes continuous climbing with all four motors operating near the estimated load. In typical operation, the drivetrain is only intermittently engaged during ascent or repositioning, while extended sensing phases require little actuation. During descent, gravitational assistance further reduces torque demand and motor current, lowering the effective energy consumption relative to this worst-case estimate. Lower gear ratios (e.g., 30:1 or 15:1) on future TetherBot versions could increase climbing speed while satisfying torque and current limits.

C. Integrated Sensing Capabilities

The TetherBot integrates environmental and navigation sensors (see Table I) to capture variables governing near-surface atmospheric processes and locomotion performance. This multi-sensor suite enables concurrent monitoring of meteorological, trace gas, and positional data, with redundancy across modalities (e.g., GNSS vs. pressure for altitude). Sensors were selected to balance SWaP constraints and accuracy while supporting shared digital buses (I^2C, SPI, UART) and co-located sampling for cross-calibration.

1) Inertial Measurement Unit (IMU): A six-axis ST LSM6DSO IMU provides linear acceleration and angular velocity for tilt correction and locomotion diagnostics. Operating at 50–100 Hz, it supplies motion context while maintaining low computational load. Redundancy is not required because the IMU serves primarily as a supportive diagnostic sensor rather than a core environmental measurement.

2) Thermistor: High-precision bead thermistors (Semitec 203AP-2, 20 kΩ) measure ambient temperature via an external SPI ADC (MCP3008). Triplicate sensors allow median filtering to reject faulty readings and improve robustness. Fast response in aspirated airflow enables detection of transient gradients and provides reference for humidity sensing.

3) Pressure Sensor: Bosch BMP581 sensors measure barometric pressure with ± 0.5 Pa accuracy (centimeter-scale altitude resolution). Three units are distributed across I^2C multiplexer channels to provide redundancy and consensus filtering. Because aspiration can bias static pressure, the sensors remain passively exposed. Pressure also provides an independent check against GNSS altitude.

4) Relative Humidity Sensor: Sensirion SHT45 sensors measure humidity through diffusion with factory calibration and high accuracy. Three redundant sensors are isolated on multiplexer channels to avoid address conflicts, while active aspiration accelerates response to changing conditions. Co-location with thermistors supports joint interpretation of temperature–humidity dynamics.

5) CO_2 Sensor: The SenseAir Sunrise NDIR CO_2 sensor provides 400-5000 ppm coverage with low power consumption. Aspiration reduces diffusion lag, and co-location with temperature and humidity sensors ensures simultaneous sampling of the same air parcel. Dual-wavelength detection and baseline correction improve measurement stability.

6) Active Sensor Aspiration: To reduce diffusion lag, compact micro-blowers (Pelonis AGB154) drive $\sim$1 m/s airflow through two ducts: one for redundant thermistors and humidity sensors and another for the NDIR analyzer. Aspiration reduces humidity response time to 1-2 s and limits solar heating effects, while reducing CO_2 equilibration lag to ≤ 15 s during climbs and descents. Barometers remain unaspirated to preserve static accuracy. Although compact NDIR sensors remain noise-limited, the architecture supports future integration of higher-fidelity analyzers for boundary-layer and surface–atmosphere exchange studies.

D. Integrated Wireless Capabilities

Reliable wireless communication and positioning are essential for the TetherBot platform. The system integrates a low-power 2.4 GHz transceiver for telemetry and a multi-constellation GNSS receiver for geolocation and timing. Together, these components enable coordination between the TetherBot, the ground station, and external references.

1) Telemetry: A Nordic nRF24L01+ transceiver provides real-time data streaming in the 2.4 GHz ISM band. Interfaced via SPI, it supports configurable data rates (250 kbps-2 Mbps) and uses the Enhanced ShockBurst protocol for reliable low-power packet transmission. The link enables continuous streaming of sensor data and reception of ground-station commands for centralized monitoring and control.

2) GNSS Receiver and Antenna Integration: A u-blox MAX-M10M GNSS module provides geolocation and timing using concurrent GPS, Galileo, BeiDou, and GLONASS reception. Integrated over I^2C, with a backup UART for configuration, the receiver improves positional robustness under partial sky occlusion while providing absolute timing for sensor synchronization. The module's pulse-per-second (PPS) output triggers MCU interrupts to align all data streams with GNSS-derived Coordinated Universal Time (UTC), enabling comparison with external systems such as EC towers or weather stations. Reliable timing under strict payload constraints motivated the integration of a Maxtena M1575HCT-15A active helical antenna. The 50 Ω SMA-connected antenna includes a low-noise amplifier for improved signal acquisition under canopy or clutter while drawing modest DC current from the receiver bias line. The architecture also remains compatible with higher-precision RTK (e.g., u-blox ZED-F9P).

E. Onboard Non-volatile Data Storage

To complement wireless telemetry, the TetherBot integrates a micro Secure Digital (SD) card (via SPI) for onboard logging of raw sensor data, calibration files, and diagnostics. This provides gigabyte-scale storage and preserves complete records even if wireless links degrade or operations extend beyond radio range. Potential link degradation does not reflect a weakness in the centralized architecture but instead acknowledges realistic field conditions such as electromagnetic interference near the multi-rotor, temporary occlusions, or adverse RF environments. The nRF-based radio link typically provides $\sim$ 100 m LoS range at the configured transmit power, which is sufficient for deployments of this scale. Onboard logging serves as a resilience mechanism to ensure sensor data is preserved during brief periods of interference or antenna misalignment. All measurements are hardware-timestamped using the aforementioned robust GNSS PPS UTC pipeline. This enables synchronized time-series comparison with external platforms such as EC towers.

F. Power Budget and Distribution

The estimated upper ceiling power budget for the entire system can be seen in Table II. The TetherBot is powered by an 11.1V LiPo and is regulated into distinct power rails:

- **6V rail:** Buck-regulated for the H-bridge motor stage (peak $\sim$817 mA at $\sim$51% drivetrain stall).
- **4V rail:** Buck-regulated for aspiration micro-blowers ($\sim$45 mA each estimated with slight overdrive).
- **3.3V rail:** Low Dropout-regulated for MCU, sensors, telemetry, GNSS, and storage.

TABLE II: Estimated power budget for TetherBot subsystems.

Subsystem	I (mA)	Notes
3.3V domain (logic/sensors)		
ATMEGA328P MCU	15	Active, 8 MHz
nRF24L01+	12	TX at 0 dBm
u-blox MAX-M10M	15-40	Passive vs. active antenna
SenseAir Sunrise CO_2	35	Measurement active
BMP581 (3×)	3	$\sim$1 mA each
SHT45 (3×)	3	$\sim$1 mA each
Thermistors (3×)	1	Divider bias
LSM6DSO IMU	1	104 Hz ODR
MCP3008 ADC	1	SPI active
TCA9548A mux	1	Channel select
LEDs (4×)	20	$\sim$5 mA each
MicroSD	30	During write
Subtotal (3.3V)	137-162	Antenna choice dependent
4V domain (aspiration blowers)		
Micro-blowers (2×)	90	$\sim$45 mA each
6V domain (motors)		
Motors (4×) + H-bridge	817	$\sim$51% stall climb load
Total Output Power	—	$\sim$5.71-5.79 W

Each regulator stage includes bulk capacitance, with local decoupling at ICs to suppress transients and preserve clean rails for RF and analog subsystems. The logic domain (3.3V) draws $\sim$137-162 mA, the aspiration domain (4V) draws $\sim$90 mA total, and the motor domain (6V) peaks near $\sim$817 mA during sustained climbing. These correspond to approximate per-rail power draws of $\sim$0.45-0.53 W (3.3V), $\sim$0.36 W (4V), and $\sim$4.90 W (6V), yielding a total estimated output power of $\sim$5.71-5.79 W under sustained functional operation. For an 11.1V, 450 mAh LiPo battery, this corresponds to an ideal equivalent battery current of $\sim$520 mA and a nominal runtime near 52 minutes under continuous peak load. Accounting for regulator inefficiencies, usable-capacity limits, and non-ideal discharge behavior, a conservative continuous-actuation and sensing runtime is on the order of 35-45 minutes. In practice, the drivetrain is intermittently engaged and descent imposes a reduced mechanical load. Typical mission durations are therefore expected to exceed this conservative bound.

G. Embedded Architecture and Firmware

The TetherBot embedded system uses a modular motherboard–daughterboard PCB architecture. The daughterboard integrates power regulation, motor drivers, and aspiration blower control, isolating high-current switching from the sensing and logic domain. The motherboard hosts the 8-bit MCU (8 MHz external crystal), which manages motor actuation, sensor acquisition, telemetry, and onboard logging. GNSS hardware UTC timestamping anchors all data streams. The boards are electrically coupled through a star-ground connection and linked via Molex Micro-Lock assemblies to reduce common-impedance noise. Shared buses (I^2C, SPI, UART) support multi-sensor integration with appropriate grounding and decoupling. Typical sampling rates are 1–10 Hz for PTH and CO_2, and 50–100 Hz for the IMU, keeping computational load well within MCU capacity. Key environmental variables such as PTH are measured using triplicate sensors, enabling median-based consensus filtering to mitigate drift or single-sensor failure. I^2C address

conflicts among redundant sensors (e.g., SHT45, Sunrise CO_2) are resolved with a TCA9548A multiplexer, while additional analog thermistors and system-monitoring inputs are expanded through an MCP3008 SPI 10-bit ADC. Together, multiplexing, ADC expansion, and consensus filtering allow the MCU to manage the redundant sensor suite efficiently while buffering SD writes and streaming telemetry at 250 Kbps–2 Mbps.

Firmware operation is governed by a lightweight control loop integrating sensing, state estimation, locomotion, and safety monitoring (see Algorithm 1). The controller operates as a two-state finite automaton governing vertical motion with discrete *ASCENT* and *DESCENT* states. At each iteration, redundant PTH measurements are reconciled through consensus filtering, while altitude is estimated using multi-sensor fusion of GNSS, barometric pressure, and IMU measurements. Vertical motion commands are generated using a proportional–derivative (PD) control law operating on altitude error $err(t)$ relative to the commanded profile envelope. The gains K_P and K_D were tuned empirically to ensure stable tracking of altitude setpoints while suppressing oscillations from tether tension, drivetrain inertia, and aerodynamic disturbances. The resulting vertical velocity command V_z is translated by the MCU into PWM signals delivered from the motherboard to the daughterboard H-bridge drivers controlling the drivetrain motors. Mission execution follows a repeated profiling cycle bounded by alt_{min} and alt_{max}, where $alt_{min} = 0$ defines a local reference frame origin rather than absolute ground level. Transitions between *ASCENT* and *DESCENT* occur when the estimated altitude crosses these bounds, with a small hysteresis margin (ε) preventing rapid switching. Measurements, including CO_2, are GNSS-UTC timestamped, logged locally, and transmitted via telemetry. Independent of the control loop, forward and rear LiDAR sensors are polled at an interval Δt to detect obstacles or boundary violations, terminating the mission.

Algorithm 1: TetherBot Vert. Profiling Control Loop

```
mission_end ← false;
phase ← ASCENT;
alt_min(t) ← 0;
alt_max(t) ← target_alt;
profiles_done ← 0;
profiles_target ← N;
// --Initialization--
Sync clock ← GNSS.PPS UTC;
Initialize logs, filters;
last_lidar_check ← now;
while ¬mission_end do
    // --Always sense, fuse, and log--
    [P,T,H] ← f_consensus({P_i,T_i,H_i});
    alt_est(t) ← f_fusion(GNSS,Barometer,IMU);
    Read CO_2, IMU; Timestamp ← GNSS.UTC;
    Log+TX {P,T,H,CO_2,IMU,alt_est,Timestamp};
    // --Vertical profiling control--
    switch phase do
        case ASCENT do
            err(t) ← alt_max(t) - alt_est(t);
            V_z(t) ← K_P · err(t) + K_D · d/dt err(t);
            if alt_est(t) ≥ alt_max(t) - ε then
                phase ← DESCENT;
        case DESCENT do
            err(t) ← alt_min(t) - alt_est(t);
            V_z(t) ← K_P · err(t) + K_D · d/dt err(t);
            if alt_est(t) ≤ alt_min(t) + ε then
                phase ← ASCENT;
                profiles_done ← profiles_done + 1;
                if profiles_done ≥ profiles_target then
                    mission_end ← true;
    // --Periodic boundary check--
    if now - last_lidar_check ≥ Δt then
        Read forward/rear LiDAR sensors;
        if obstacle then
            mission_end ← true;
        last_lidar_check ← now;
```

IV. Field Experiments

This section outlines the experimental deployment of the TetherBot-enabled TAUS platform in the wild. Experiments were conducted at Rogers Memorial Farm (RMF), which provides a representative agroecosystem setting. Deployments took place during calm weather conditions at sunset on several evenings in early September 2025. An open grass section of the farm, adjacent to a mature cornfield and a ground-based meteorological station, was selected for the experiment. At this time of year, the corn crop remained standing and actively transpiring, forming a dense canopy that influences near-surface humidity and temperature structure and provides a realistic agricultural boundary-layer environment for atmospheric sensing experiments. The TetherBot was mounted onto the power tether $\sim$10 m below the hoisting sUAS. Once armed, the sUAS elevated the tether to a target altitude of 20 m above ground level (AGL), stabilizing its position using onboard IMU and GNSS feedback. During active deployment, the TetherBot collected and time-synchronized atmospheric measurements while relaying data packets in near-real time and executing the autonomous sensing and motion phases defined by the control loop. To provide an independent aerial reference, a hexacopter based on the F550 airframe and equipped with a CubePilot Blue FMU was retrofitted with an iMet-X4 PTH sensor suite. The iMet-X4 housing incorporates an extended intake designed to sample air outside the immediate rotor wash region, reducing propeller-induced turbulence and improving PTH sampling fidelity. This configuration reflects a non-trivial, platform-specific mitigation strategy to reduce rotor-induced perturbations, consistent with prior work on sUAS-based atmospheric sensing. The F550 sUAS was flown to 10 m AGL, matching the initial altitude of the TetherBot, and maintained position

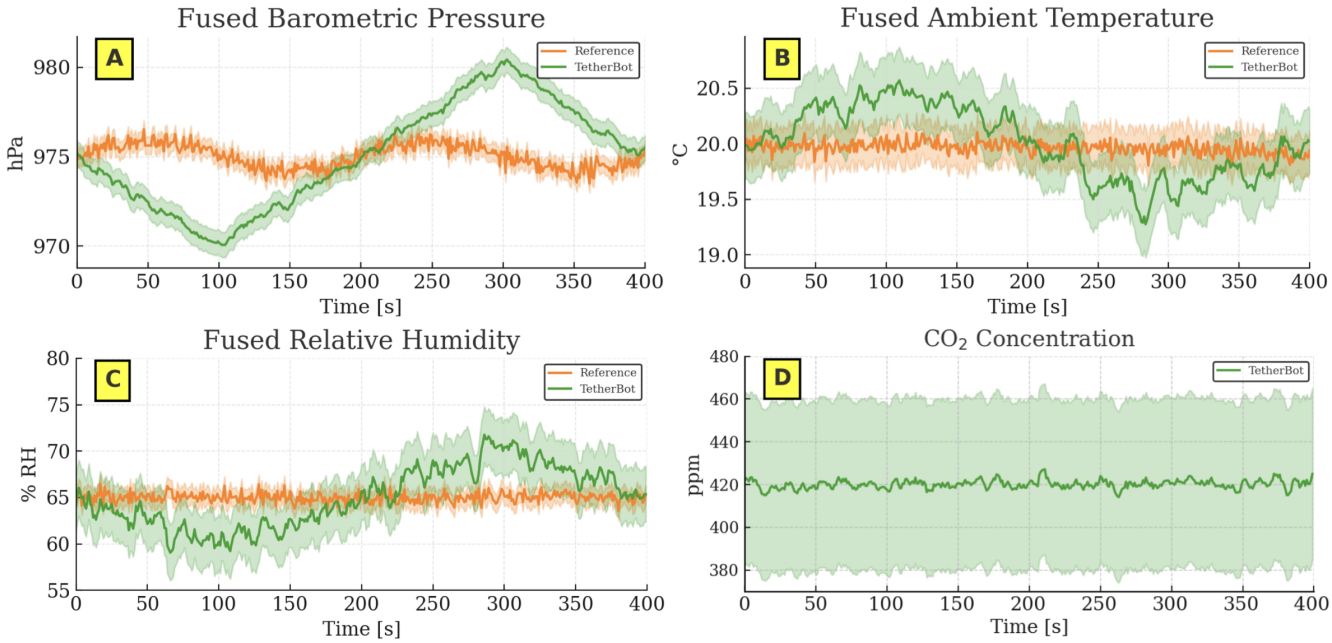

Fig. 4: Fused state variables during TetherBot profiling. (A) Barometric pressure exhibits the clearest vertical response with a narrow reference noise envelope. (B) Ambient temperature reveals a mild inversion, with stable reference measurements and modest TetherBot variation. (C) Relative humidity shows the strongest variability, with a jagged envelope reflecting sensor noise and ecosystem humidity dynamics. (D) CO_2 concentration centers near 420 ppm but is dominated by a broad noise envelope (380–460 ppm), obscuring gradients.

in proximity throughout the experiment while the TetherBot traversed between ∼0-20 m. The TetherBot executed repeated ascent–descent cycles during the experiment. Each vertical profiling cycle began at 10 m AGL and consisted of a 10 m ascent to 20 m, followed by a 20 m descent to 0 m local reference frame origin, and a final 10 m ascent returning to 10 m. This sequence produced a total vertical traversal distance of ∼40 m per cycle. Rotation about the tether during traversal was incidental and resulted from the natural torsional compliance of the power tether and minor mass imbalances in the robot rather than any active control effort to achieve or maintain a specific orientation. The robot maintained an average vertical speed of ∼0.1 m/s during both ascent and descent. Although the total vertical travel distance reached 40 m, the maximum separation between the robot and the radio base station remained on the order of 20 m.

V. Results

TetherBot produced continuous time-series measurements of barometric pressure, ambient temperature, relative humidity, and CO_2 concentration while executing repeated 40 m vertical transects. Across all variables, the TetherBot record exhibited larger variability and broader signal envelopes than the quasi-stationary aerial reference platform (F550 iMet-X4). This reflects both vertical atmospheric gradients and sensor-induced variability. Standard deviation (σ), variance (σ^2), and signal-to-noise ratio (SNR) statistics were computed for each signal. Here, SNR is defined as the ratio between the observed signal amplitude $\mathscr{A}$ and the standard deviation of the measurements ($\mathrm{SNR} = \mathscr{A}/\sigma$). The resulting statistics aid the interpretation of the plotted data (see Fig. 4). Together, these metrics provide a quantitative framework for distinguishing environmental structure from sensor-induced variability across the vertical profile.

Barometric pressure provided the clearest vertical response (see Fig. 4: Panel A). The TetherBot profile varied smoothly by ∼8 hPa across the transect, following the imposed motion phases dictated by Algorithm 1. The reference remained stable near 975 hPa with $\sigma \approx 0.4$ hPa, while the TetherBot variability ($\sigma \approx 2.59$ hPa, $\sigma^2 \approx 6.7$ hPa^2, SNR ≈ 3.09) reflected the imposed altitude excursions rather than measurement noise alone. These results confirm fused barometric pressure as a stable and reliable observable for vertical structure estimation. Ambient temperature revealed a mild inversion, typical of near-sunset conditions (see Fig. 4: Panel B). While the reference remained flat near 20 °C ($\sigma \approx$ 0.2 °C), the TetherBot record swung by ∼1 °C. Variability ($\sigma \approx 0.71$ °C, $\sigma^2 \approx 0.5$ °C^2, SNR ≈ 1.41) exceeded the reference but still highlighted subtle stratification even across a limited altitude range. Relative humidity exhibited the strongest variability (see Fig. 4: Panel C). The reference hovered near 65% ($\sigma \approx 1.1\%$), while the TetherBot swung from 60-75%. Variability ($\sigma \approx 3.39\%$, $\sigma^2 \approx 11.5\%^2$, SNR ≈ 4.42) reflected both environmental structure and sensor noise, yet the profile clearly distinguished drier air aloft from the more humid microclimate near the vegetated canopy. CO_2 centered near 420 ppm, consistent with atmospheric background, but was dominated by a wide uncertainty band between 380-460 ppm (see Fig. 4: Panel D). Variability ($\sigma \approx 15.81$ ppm, $\sigma^2 \approx 250$ ppm^2) remained high relative to expected canopy-scale gradients. Under calm near-sunset conditions typical of agricultural boundary layers, vertical

CO_2 gradients over the lowest 10-20 m are commonly on the order of only a few ppm to roughly $\sim$10 ppm. Using this conservative estimate as the characteristic signal amplitude yields an SNR $\approx 10/15.81 \approx 0.63$. Since SNR < 1, the expected atmospheric signal is smaller than the intrinsic measurement variability, masking subtle vertical gradients. This indicates that the aspirated NDIR sensor, rather than the mobile profiling platform, was the dominant limiting factor in resolving vertical CO_2 structure.

VI. Conclusion

This work presented the design, integration, and initial field validation of the TetherBot-enabled TAUS platform for atmospheric sensing in agroecosystems. The system combines a ground station, an sUAS-hoisted power tether, and a compact mobile robot to enable persistent vertical profiling with synchronized sensing and telemetry. Through a streamlined embedded architecture, redundant sensors, and active aspiration, the platform demonstrates that lightweight robotic systems can resolve fine-scale atmospheric gradients under field conditions. Results from a 40 m profiling deployment confirmed barometric pressure as a stable anchor for altitude estimation, temperature as a marker of subtle stratification, and relative humidity as an indicator of pronounced surface-layer variability. In contrast, CO_2 measurements were dominated by sensor variability, highlighting the limitations of compact NDIR sensors when resolving gradients on the order of only a few ppm. Such sensors are well-suited for applications like HVAC monitoring, but their intrinsic noise makes resolving subtle canopy-scale gradients challenging. The TetherBot was benchmarked against an independent aerial reference, a hexacopter built on an F550 airframe carrying an aspirated iMet-X4 PTH suite that provided quasi-stable measurements at 10 m AGL for baseline comparison. While this reference employs mitigation strategies to reduce platform-induced disturbances, the TetherBot architecture avoids such effects through mechanical decoupling. By linking compact robotic mobility with atmospheric sensing, this work demonstrates how autonomous platforms can complement existing environmental monitoring infrastructure and improve observation of surface–atmosphere exchange.

Future work will address limitations by extending this framework through coordinated multi-robot operation and integration of higher-fidelity gas analyzers to support advanced flux measurements. Additional deployments will target higher altitudes, broader conditions, and longer durations. Distributed communication strategies may further extend operational range and maintain connectivity in more challenging environments. Together, these extensions support more comprehensive observation of carbon and energy dynamics in agroecosystems while preserving the lightweight robotic architecture demonstrated in this work.

Acknowledgments. We would like to thank the University of Nebraska-Lincoln, North Carolina State University, NIMBUS, AERIS, and CAASA Laboratories, Rogers Memorial Farm, Daugherty Water for Food Global Institute, Benjamin W. Moll and Adam L. Houston for their assistance with F550 iMet-X4 sensing, and Jocelyn M. Kennicutt for her support in facilitating timely procurement of hardware resources.

References

[1] R. Lal, "Soil carbon sequestration to mitigate climate change," *Geoderma*, vol. 123, pp. 1–22, Nov. 2004.

[2] N. Academy of Sciences, *Negative Emissions Technologies and Reliable Sequestration: A Research Agenda*. National Academies Press, Apr. 2019. Google-Books-ID: owONDwAAQBAJ.

[3] T. Foken, "The Energy Balance Closure Problem: An Overview," *Ecological Applications*, vol. 18, no. 6, pp. 1351–1367, 2008. _eprint: https://esajournals.onlinelibrary.wiley.com/doi/pdf/10.1890/06-0922.1.

[4] T. M. Bell, B. R. Greene, P. M. Klein, M. Carney, and P. B. Chilson, "Confronting the boundary layer data gap: evaluating new and existing methodologies of probing the lower atmosphere," *Atmospheric Measurement Techniques*, vol. 13, pp. 3855–3872, July 2020. Publisher: Copernicus GmbH.

[5] P. J. Hardin, V. Lulla, R. R. Jensen, and J. R. Jensen, "Small Unmanned Aerial Systems (sUAS) for environmental remote sensing: challenges and opportunities revisited," *GIScience & Remote Sensing*, vol. 56, pp. 309–322, Feb. 2019. Publisher: Taylor & Francis _eprint: https://doi.org/10.1080/15481603.2018.1510088.

[6] A. Islam, A. L. Houston, A. Shankar, and C. Detweiler, "Design and Evaluation of Sensor Housing for Boundary Layer Profiling Using Multirotors," *Sensors*, vol. 19, p. 2481, Jan. 2019. Publisher: Multidisciplinary Digital Publishing Institute.

[7] M. Sulkava, S. Luyssaert, S. Zaehle, and D. Papale, "Assessing and improving the representativeness of monitoring networks: The European flux tower network example," *Journal of Geophysical Research: Biogeosciences*, vol. 116, no. G3, 2011. _eprint: https://agupubs.onlinelibrary.wiley.com/doi/pdf/10.1029/2010JG001562.

[8] M. Dunbabin and L. Marques, "Robots for Environmental Monitoring: Significant Advancements and Applications," *IEEE Robotics & Automation Magazine*, vol. 19, pp. 24–39, Mar. 2012.

[9] R. P. Pratama, A. Rusdinar, and I. P. D. Wibawa, "Floating Robot Control System for Monitoring Water Quality Levels in Citarum River," in *2019 IEEE International Conference on Internet of Things and Intelligence System (IoTaIS)*, pp. 206–211, Nov. 2019.

[10] X. Lyu, X. Li, D. Dang, H. Dou, K. Wang, and A. Lou, "Unmanned Aerial Vehicle (UAV) Remote Sensing in Grassland Ecosystem Monitoring: A Systematic Review," *Remote Sensing*, vol. 14, p. 1096, Jan. 2022. Publisher: Multidisciplinary Digital Publishing Institute.

[11] S. Khemiri, M. A. Kishk, and M.-S. Alouini, "Exploiting tethered and untethered UAVs: a hybrid aerial communication system," *Scientific Reports*, vol. 15, p. 15882, May 2025. Publisher: Nature Publishing Group.

[12] A. Borgese, D. C. Guastella, G. Sutera, and G. Muscato, "Tether-Based Localization for Cooperative Ground and Aerial Vehicles," *IEEE Robotics and Automation Letters*, vol. 7, pp. 8162–8169, July 2022.

[13] J. Katrasnik, F. Pernus, and B. Likar, "A Survey of Mobile Robots for Distribution Power Line Inspection," *IEEE Transactions on Power Delivery*, vol. 25, pp. 485–493, Jan. 2010.

[14] F. Xu, S. Dai, Q. Jiang, and X. Wang, "Developing a climbing robot for repairing cables of cable-stayed bridges," *Automation in Construction*, vol. 129, p. 103807, Sept. 2021.

[15] M. Xu, W. Tian, Y. Lin, Y. Xu, and J. Tao, "Development of a Compact NDIR CO2 Gas Sensor for a Portable Gas Analyzer," *Micromachines*, vol. 15, p. 1203, Sept. 2024.

[16] T. J. Schuyler and M. I. Guzman, "Unmanned Aerial Systems for Monitoring Trace Tropospheric Gases," *Atmosphere*, vol. 8, p. 206, Oct. 2017. Publisher: Multidisciplinary Digital Publishing Institute.

[17] D. A. Rico, F. Munoz-Arriola, and C. J. Detweiler, "Power-over-Tether UAS Leveraged for Nearly-Indefinite Meteorological Data Acquisition," *American Society of Agricultural and Biological Systems Engineering (ASABE)*, July 2020.

[18] D. A. Rico, F. Munoz-Arriola, and C. J. Detweiler, "Trajectory Selection for Power-over-Tether Atmospheric Sensing UAS," in *IEEE/RSJ International Conference on Intelligent Robots and Systems (IROS)*, (Prague, Czech Republic), pp. 2321–2328, IEEE, Sept. 2021.

[19] D. A. Rico, F. Muñoz-Arriola, J. M. Bradley, and C. J. Detweiler, "Analytics for Real-Time Inertial Localization of the Tethered Aircraft Unmanned System," in *International Symposium on Experimental Robotics (ISER)* (M. H. Ang Jr and O. Khatib, eds.), (Cham), pp. 469–480, Springer Nature Switzerland, Nov. 2024.